Development of Wide Operating Temperature Range (–30～70℃) Athermal AWG Module with High Reliability

*by Junichi Hasegawa * and Kazutaka Nara **

ABSTRACT The authors have clarified the cause of the temperature dependence in athermal Arrayed Waveguide Grating (AWG) modules of conventional type, and have developed a new athermal AWG module of wide operating temperature range having a reduced temperature dependence. The temperature dependence of the center wavelength of the developed module is not more than ±0.015 nm for all channels over a temperature range of –30～70℃. A series of reliability tests have been carried out assuming outdoor installation of the module, and it has been confirmed that the module has extremely high reliability.

1. INTRODUCTION

Athermalization, or realization of temperature independence, of arrayed waveguide gratings (AWGs) which handle the function of wavelength multiplexing/demultiplexing has become an indispensable requirement for constructing optical communications networks that are ever diversifying. To satisfy the demand, we have devised proprietary athermalization principles, and have developed a number of athermal AWG modules [1)~3)]. And now, in recent years, the next-generation communications system based on Wavelength Division Multiplexing – Passive Optical Network (WDM-PON) scheme is being intensively studied especially in Korea. In this system, it is possible to offer each user an independent transmission method and speed, because different wavelengths are assigned to each user by using a wavelength multiplexer/demultiplexer. A number of approaches have been reported so far to use AWG modules as wavelength multi/demultiplexers [4), 5)] taking advantage of the ease of channel multiplication and mass production of AWGs.

Figure 1 shows a schematic diagram of WDM-PON system. As shown, the AWG modules are installed outdoors, e.g. in a closure, like optical splitters used in ordinary PON systems. For this reason, the AWG modules are required to be provided with such characteristics as athermalization and high reliability in addition to a wide operation temperature range of –30～70℃. In response to the requirement of improving the operation temperature range, we have theoretically clarified the cause of the slight temperature dependence in athermal AWGs of conventional type, and have developed a new athermal AWG module that has achieved a reduced temperature dependence of the center wavelength. This paper reports on the development together with the results of reliability tests on the module in which, as a result of the tests conducted assuming outdoor installation, it has been confirmed that the module has high reliability.

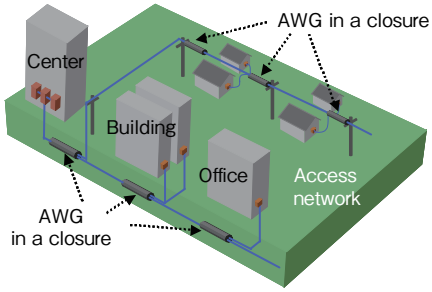

Figure 1 Schematic diagram of WDM-PON system.

2. CAUSE CLARIFICATION OF TEMPERATURE DEPENDENCE OF CENTER WAVELENGTH IN CONVENTIONAL ATHERMAL AWG MODULE

2.1 Structure and Temperature Dependence of Conventional Athermal AWG Module

Figure 2 (a) is the simplified structural diagram of a conventional athermal AWG. The AWG chip is cut at one of the slab waveguides, and each AWG chip is connected with a compensating plate made of copper. As temperature changes the copper plate expands and contracts, causing the position of the output waveguides to shift. Figure 2 (b) schematically shows the mechanism of temperature compensation. In a temperature-controlled AWG, if not temperature controlled, the focus point will shift as

* FITEL-Photonics Lab., R&D Div.

the temperature fluctuates causing the center wavelength to change. In an athermal AWG, on the other hand, the focus point will also shift as the temperature fluctuates, but the expansion or contraction of the copper plate moves the output waveguides to the new focus point, so that the center wavelength is compensated. The shift distance is adjustable by the length of the copper plate.

Figure 3 shows the temperature dependence of the center wavelength of the conventional athermal AWG. The temperature dependence is slightly convex downward, and the temperature dependence of the center wavelength is less than ±0.015 nm over a temperature range of -5~70℃ specified in the general specification for office applications. The dependence will be greater when the operation temperature range is expanded, becoming not negligible in actual use. Thus, in order for the AWG module to be applied in WDM-PON systems where expansion of operation temperature ranges is needed, the temperature dependence of the AWG center wavelength has to be reduced further.

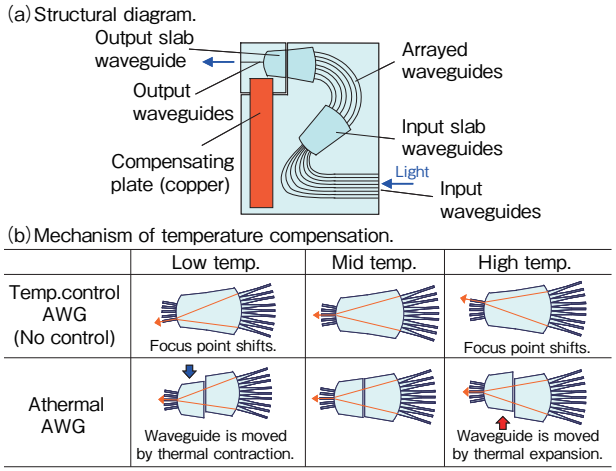

Figure 2 Outline of athermal AWG.

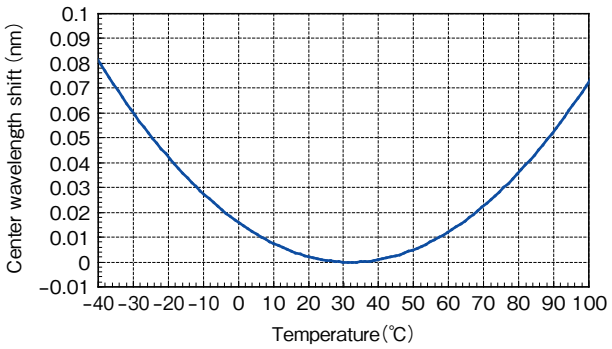

Figure 3 Temperature dependence of conventional athermal AWG center wavelength.

2.2 Theoretical Investigation Concerning the Cause of the Downward-Convex Temperature Dependence of Center Wavelength

To begin investigation as to the cause why the temperature dependence of the center wavelength shows a downward-convex curve, we focused our attention on the temperature dependence of the refractive index of silica-based material, which is supposed to contribute a great deal to the temperature dependence. In general, the temperature dependence of the refractive index of silica-based material is expressed as $dn/dT \fallingdotseq 8 \times 10^{-6}$, a constant. However, it is reported that the temperature dependence of the refractive index does not take a constant value in actuality, but changes as a function of temperature T [6]. Thus, the refractive index n of silica-based material including its temperature dependence is expressed by the Sellmeier polynomial formula as shown in Equation (1).

$$n = \sqrt{1 + \sum_{i=1}^{3} \frac{a_i}{b_i^2 - \left(hc/\lambda\right)^2}} \qquad (1)$$

where: h is Planck's constant; c is the light velocity; λ is the wavelength; a_i and b_i are Sellmeier parameters considering temperature characteristics as shown in Equation (2). a_i is dependent on the oscillator strength and number of oscillators per unit volume, while b_i is dependent on the resonance energy of the oscillators.

$$a_i = a_{i0} + a_{i1}T + a_{i2}T^2$$
$$b_i = b_{i0} + b_{i1}T + b_{i2}T^2 \qquad (2)$$

These parameters are shown in Table 1.

The temperature dependence of the refractive index of silica-based material can be calculated using Equations (1) and (2) together with Table 1, and is found to be almost linear as shown in Figure 4. This result means that the refractive index of silica-based material changes in a quadratic curve with respect to temperature.

Table 1 Sellmeier's parameters considering temperature dependence.

		i=1	i=2	i=3
a_{i0}	eV²	228.7018	46.40806	0.014173
a_{i1}	eV²/℃	4.930E-05	−3.270E-05	−1.704E-06
a_{i2}	eV²/℃²	1.100E-07	−3.780E-08	−2.140E-09
b_{i0}	eV	18.11163	10.671082	0.125
b_{i1}	eV/℃	9.150E-06	−2.991E-04	0
b_{i2}	eV/℃²	7.478E-08	−4.807E-07	0

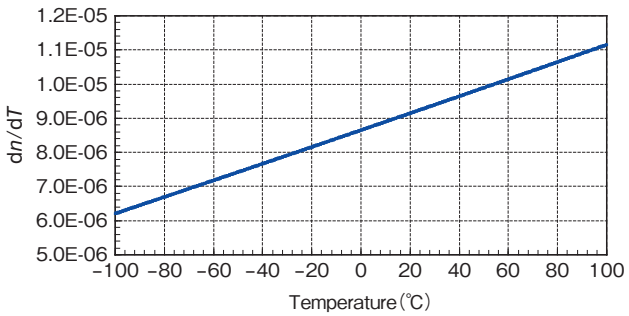

Figure 4 Temperature dependence of refractive index of silica-based material.

Next let us calculate temperature dependence of the center wavelength of an AWG using circuit parameters shown in Table 2.

Using these parameters, the center wavelength of the AWG is give by Equation (3).

$$\lambda = \frac{\Delta L}{m} n_c \tag{3}$$

To understand the temperature characteristics of center wavelength, the temperature change of n_c has to be evaluated accurately. Accordingly, we calculated the temperature change of n_c by the effective index method, letting the refractive index of the clad glass be the one obtained by Equations (1) and (2), that of the core glass be the one obtained by uniformly adding a Δ=0.8 % to that of the clad glass, and under the condition of the layer thickness and the line width being equal to 6.5 μm.

On the other hand, the athermal AWG we developed was temperature compensated almost linearly taking advantage of thermal expansion and contraction of the copper plate, where the copper plate was adjusted in length to minimize the temperature dependence of the center wavelength over a design operation temperature range of -5～70℃.

Based on the discussions described above, we have calculated the temperature dependence of the center wavelength of the AWG as well as the temperature compensation using the copper plate and, what is derived from these, the temperature dependence of the center wavelength of the conventional athermal AWG, and the results are shown in Figure 5 (a). Each result is normalized so as to correspond to a designed wavelength at 20℃. The temperature dependence of the center wavelength of the AWG changes in a quadratic curve because the temperature dependence of the refractive index of silica-based material is not constant in contrast to the fact that the temperature compensation by the copper plate changes almost linearly. This results in the temperature dependence of the center wavelength after compensation which shows a slightly downward-convex shape. It can be seen from this series of calculations that the downward-convex temperature dependence of the center wavelength of the athermal AWG is caused by the compensation mechanism, where the temperature characteristics of the center wavelength of the AWG having a quadratic curve is compensated by using the copper plate having an almost linear temperature characteristic. Meanwhile, as can be seen in Figure 5 (b), the temperature dependence obtained by calculation is in agreement with that of the center wavelength of an athermal AWG module experimentally measured.

3. LINEAR EXPANSION CHARACTERISTICS OF COMPENSATING PLATE FOR COMPLETE ATHERMALIZATION

The calculation results above mentioned implies that it is possible to athermalize an AWG if there exists a compensating plate which matches the AWG in terms of nonlinear temperature dependence of the center wavelength. We calculated the linear expansion property required for such a compensating plate. The amount of positional compensation dx to be used in the athermal AWG is given by Equation (4) using the circuit parameters shown in Table 2.

$$dx = \frac{L_f m n_g}{n_s d n_c} \left(\frac{d\lambda}{dT} \right) (T - 20) \tag{4}$$

where the temperature is expressed by a change from 20℃, and the temperature dependence of the center wavelength $d\lambda/dT$ is given by Equation (5).

$$\frac{d\lambda}{dT} = \frac{\lambda}{n_c} \left(\frac{dn_c}{dT} \right) + \lambda \alpha_s \tag{5}$$

Table 2 Circuit parameters of AWG.

Channel spacing (GHz)		100
Channel number		40
Focal length of slab waveguide (mm)	Lf	17.2
Diffraction order	m	29
Pitch of adjacent arrayed waveguide (μm)	d	13.8
Path length difference of arrayed waveguide (μm)	ΔL	31.0
Group index of arrayed waveguide at R.T.	n_g	1.4760
Effective index of slab waveguide at R.T.	n_s	1.537
Effective index of arrayed waveguide at R.T.	n_c	1.4514

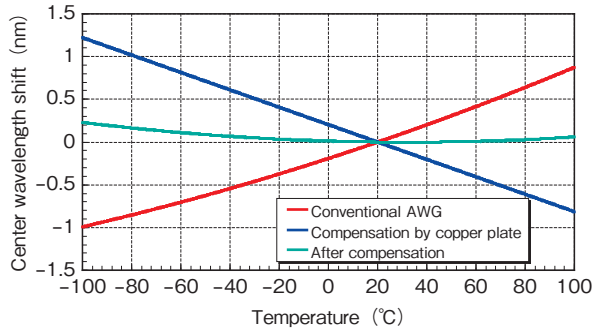

(a) Calculation result.

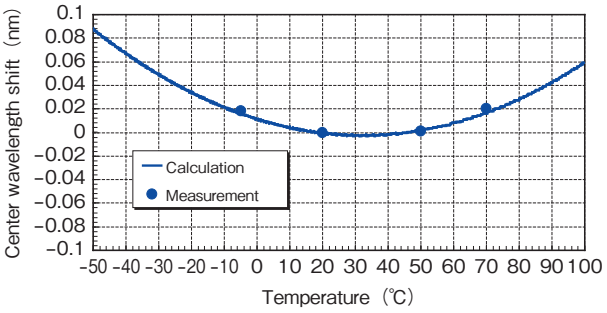

(b) Comparison with measurement result.

Figure 5 Temperature dependence of the center wavelength of conventional athermal AWG.

where α_s is the linear expansion coefficient of silicon which constitutes the substrate of the AWG, and is equal to 3.0 x 10^{-6}/℃. Figure 6 shows the amount of positional compensation dx for complete athermalization, which is calculated using Equations (4) and (5) together with Equation (3). From the Figure, it can be seen that the positional compensation dx required shows a quadrature characteristic with respect to temperature. The temperature dependence of dx, i.e. $d(dx)/dT$ is calculated as shown in Equation (6).

$$\frac{d(dx)}{dT} = (6.74 \times 10^{-4})T + 0.237 \qquad (6)$$

Selecting a material that satisfies the rate of change of $d(dx)/dT$ for a compensating plate will result in complete athermalization. Figure 7 compares the calculated rate of change, i.e. $d(dx)/dT$ with those of common metal materials, where the calculated rate of change is seen to be extremely higher than those of metal materials. Consequently, we selected an aluminum material JIS A1050 that has the highest rate of change of $d(dx)/dT$ among metal materials.

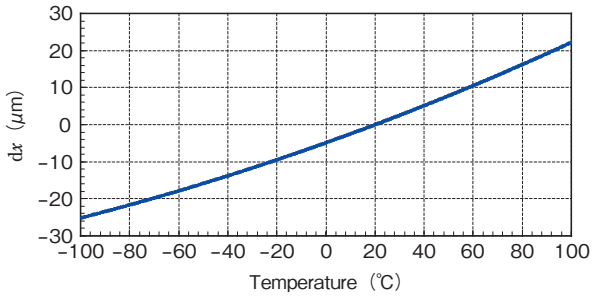

Figure 6 Calculation result of dx for complete athermalization.

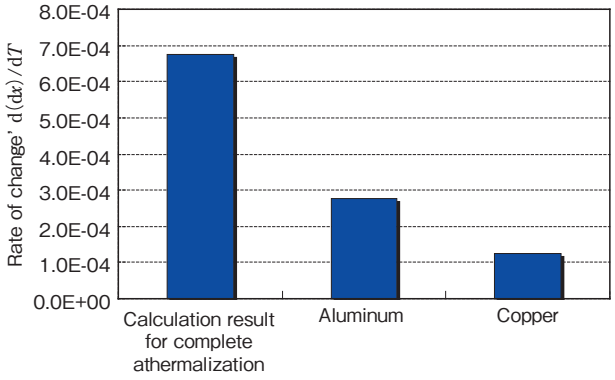

Figure 7 Comparison of the rate of change of dx/dT with metal materials.

4. FABRICATION RESULTS

Using the planar lightwave circuit (PLC) fabrication technology that combines flame hydolysis deposition (FHD), photolithography and reactive ion etching, we fabricated a 100-GHz 48-ch AWG chip. The chip was cut at the slab waveguide, and was athermalized whereby a pure aluminum plate of JIS A1050 was connected as a compensating plate. Optical fibers were then connected to the AWG chip, which was then packaged. Figure 8 shows the appearance of the athermal AWG module that was fabricated. The package was compact and slim, measuring 130 x 65 x 8.5 mm.

Figure 9 shows the spectrum of the 100-GHz 48-ch athermal AWG module. Excellent optical characteristics were obtained, with insertion loss of less than 2.5 dB (1.8~2.5 dB), and crosstalk less than -30 dB. There was no degradation of optical characteristics due to athermalization.

Figure 10 shows the temperature dependence of the center wavelength and, for the sake of comparison, that of conventional athermal AWG module using a compensating plate of copper. The temperature dependence of the AWG module using a pure aluminum compensating plate was less than ±0.015 nm over a temperature range of -30~70℃, achieving a significant reduction over the conventional. The change in insertion loss was less than ±0.1 dB. Figure 11 shows the temperature dependence of the spectrum. No spectrum degradation was observed at any of the temperatures, confirming that other optical characteristics were also stable.

Figure 8 Appearance of 100-GHz 48-ch athermal AWG module.

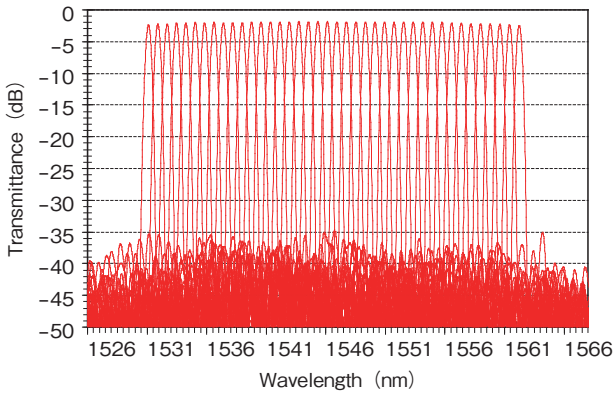

Figure 9 Spectrum of 100-GHz 48-ch athermal AWG module.

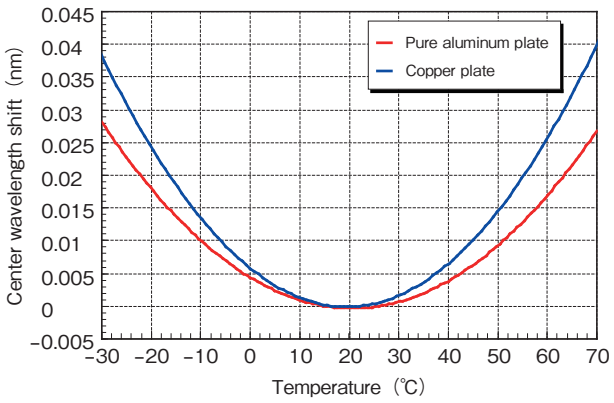

Figure 10 Temperature dependence of center wavelength.

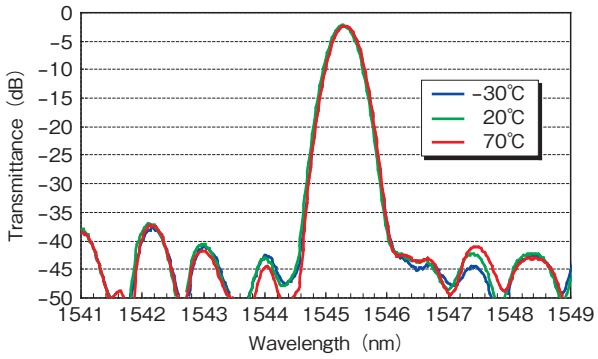

Figure 11 Temperature dependence of spectrum.

5. RELIABILITY TESTS ASSUMING OUTDOOR INSTALLATIONS

We have heretofore carried out a series of tests in conformity with Telcordia GR-1221 and GR-1209 to evaluate the reliability performance of this athermal AWG module, thereby confirming that no problems occur [1]. However, when used outdoors, the modules may be exposed to harsh environmental conditions, so that extremely high reliability is required for the modules. Accordingly, assuming all possible situations that can occur during outdoor installation, the module was tested by insertion loss monitoring tests under application of impact and vibration, water immersion tests, in addition to long-term dump heat tests and heat cycle tests lasting longer than Telcordia GR-1221.

Figure 12 shows the measuring setup for loss monitoring test. Light was input to the module using a tunable light source and a wavelength meter, and the insertion loss change was monitored for each test at a specified sampling period in the load application directions A, B and C as indicated in the Figure. Figures 13 (a) and 13 (b) show the results of impact-based loss monitoring test (50 G, 5 times, 6 directions) and vibration-based loss monitoring test (20 G, 20~2000 Hz, 4 min/cycle, 4 cycle/axis), respectively. It can be seen that no change in insertion loss occurs in each direction under the application of impact and vibration. Figure 14 shows the results of water immersion tests (43±2℃, PH5±0.5, 336 hr), in which changes from the initial values are plotted. After water immersion for 336 hours, virtually no change was observed in terms of both the center wavelength and the insertion loss. Figures 15 and 16 show the results of dump heat test (85℃, 85%RH, 5000 hr) and heat cycle test (-40~85℃, 1650 cycles), respectively. The results show that, even against these harsh tests, both the center wavelength and the insertion loss are very stable. From these test results, it has been confirmed that the athermal AWG module has extremely high reliability and that the module is rugged enough allowing for outdoor installation.

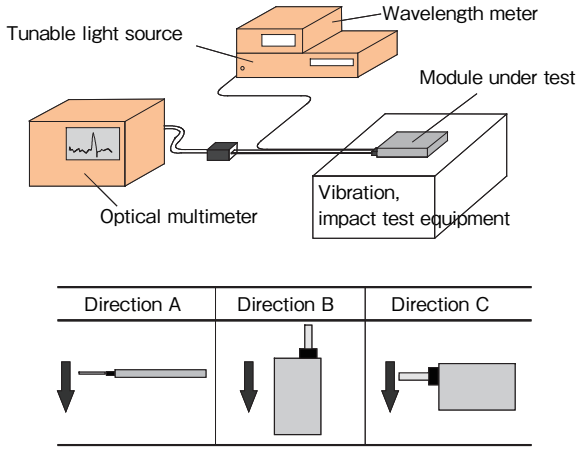

Figure 12 Outline of insertion loss monitoring test and load application directions.

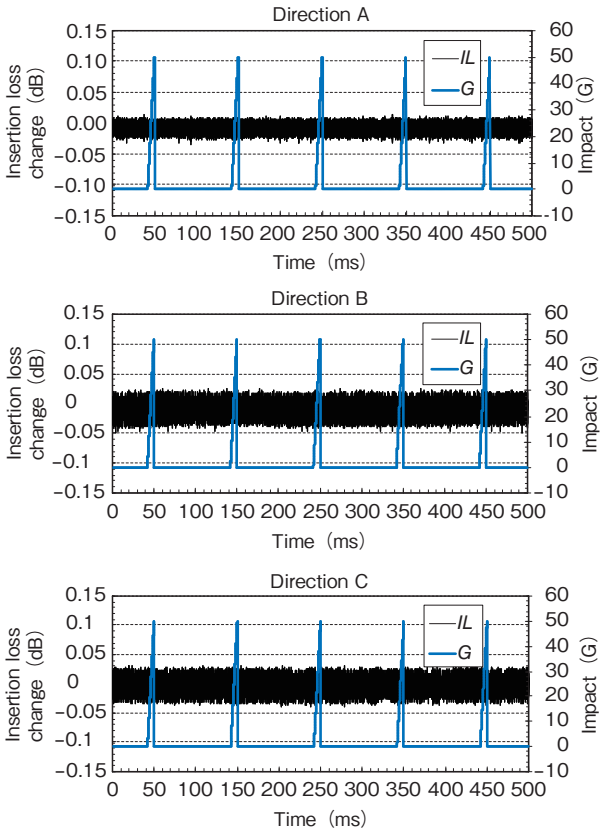

Figure 13 (a) Results of impact-based loss monitoring test.

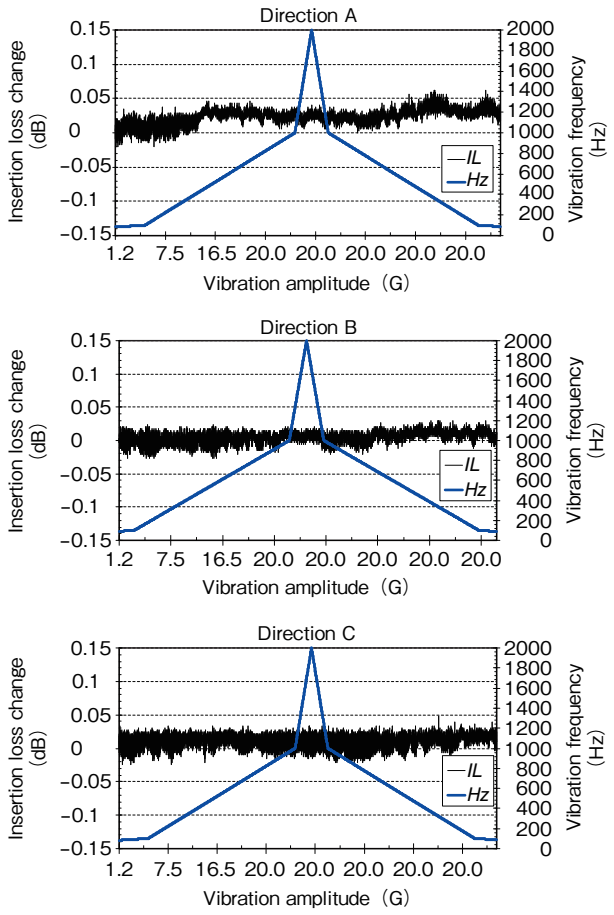

Figure 13 (b) Results of vibration-based loss monitoring test.

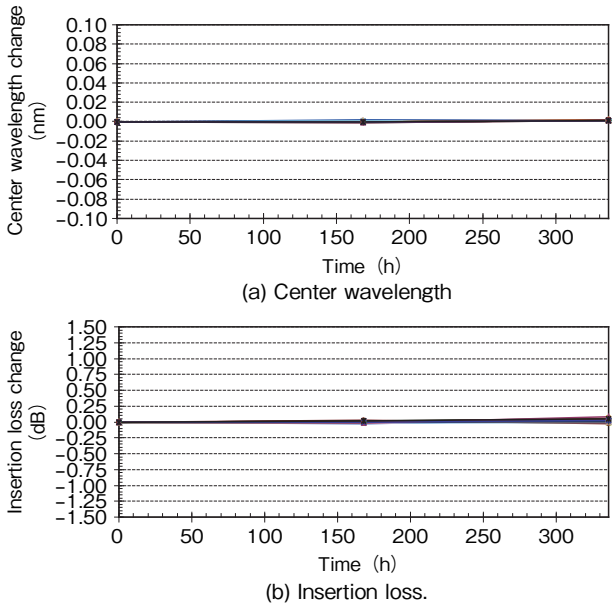

Figure 14 Results of water immersion test.

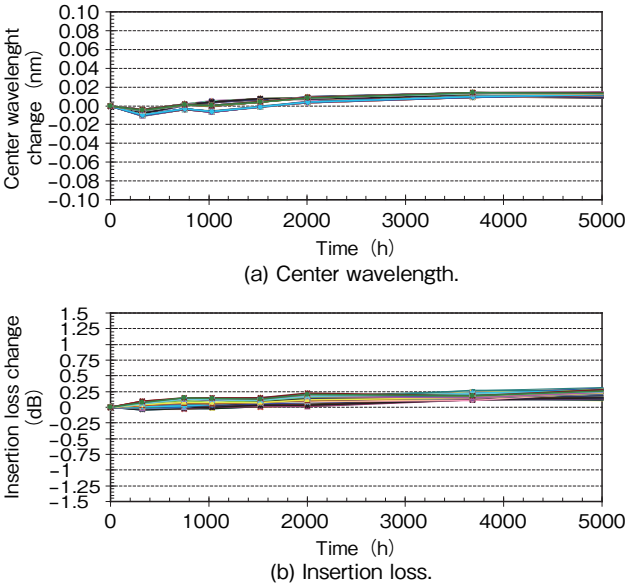

Figure 15 Results of ultra long-term dump heat test.

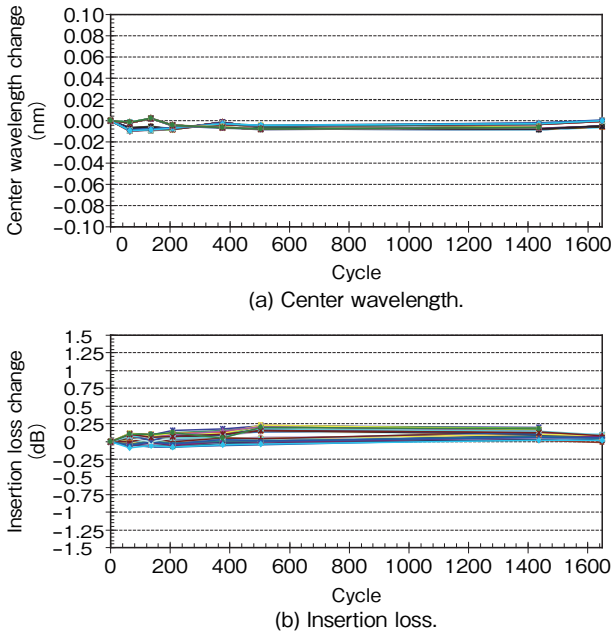

Figure 16 Results of ultra long-term heat cycle test.

6. CONCLUSIONS

We have clarified the cause of the temperature dependence in the athermal AWG module of conventional type, and have developed a new athermal AWG module with a reduced temperature dependence that permits outdoor installation. The developed module has achieved excellent performance with a temperature dependence of the center wavelength of not more than ±0.015 nm for all channels over a temperature range of -30~70℃, in addition to extremely high reliability.

REFERENCES

1) T. Saito et al.: OFC2003, MF47, (2003), 57.
2) J. Hasegawa et al.: OFC2005, OTuD5, (2005).
3) J. Hasegawa et al.: OECC2005, 7E3-3, (2005).
4) D. J. Shin et al.: OFC2005, PDP36, (2005).
5) Soo-Jin Park et al.: Journal of Lightwave Tech., 22 (2004), 2582.
6) J. Matsuda et al.: Journal of Non-Crystalline Solids, 135 (1991), 86.